

1 **A neglected anthropogenic source of carbon triggered by the**
2 **combustion of coal: evidence from riverine sulfate**

3

4

5 Ye Wang^a, Xuming Li^b, Shilei Li^a, David William Hedding^c, Jun Chen^a,
6 and Yang Chen^{a*}

7

8 ^aMOE Key Laboratory of Surficial Geochemistry, School of Earth
9 Sciences and Engineering, and Frontier Science Center for Critical Earth
10 Material Cycle, Nanjing University, Nanjing 210023, China.

11 ^b Institute for Geology, Center for Earth System Research and
12 Sustainability (CEN), Universität Hamburg, Bundesstrasse 55, 20146
13 Hamburg, Germany.

14 ^c Department of Geography, University of South Africa, Pioneer Avenue,
15 Florida 1710, South Africa.

16

17

18 * Correspondence to: Yang Chen (chenyang@nju.edu.cn)

19

20

21 **Abstract**

22

23 To effectively reduce CO₂ emissions, it's vital to identify and quantify their sources.
24 While the focus has been on CO₂ from fossil fuel combustion, especially coal, the
25 CO₂ produced from coal's other elements, such as sulfur, through chemical reaction,
26 remains an 'invisible' carbon source. Using river sulfate fluxes, we analyzed the
27 invisible carbon flux due to coal burning in the Xijiang River Basin, a highly
28 industrialized region in China. Dissolved sulfate concentration in the Xijiang River
29 rose by over 300% from 1985 to 2011, largely due to coal combustion. In 2011, this
30 resulted in 3.14 Mt of invisible carbon dioxide. We evaluated the impact of two flue
31 gas desulfurization (FGD) methods on carbon emissions with a predictive model. By
32 enhancing SO₂ removal efficiency through these methods, China could cut invisible
33 carbon emissions by 27.8 Mt CO₂ annually, paving the way for a sustainable future.

34

35 **Keywords: Climate Change, Carbon Emission, Coal Burning, Sulfur Dioxide**

36

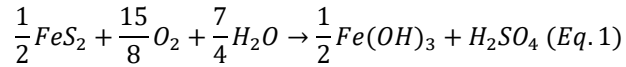
37

38

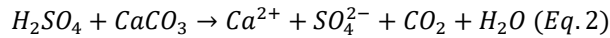
39 **Introduction**

40 Climate change is a global issue that has garnered significant attention in recent
41 years [Berrang-Ford *et al.*, 2019; Fuhrman *et al.*, 2023]. The increasing concentration
42 of greenhouse gases (GHG), especially carbon dioxide (CO₂), in the atmosphere is
43 one of the primary drivers of climate change [Andrews and Forster, 2008; Charney *et al.*, 1979]. According to the Paris Agreement (2015), governments across the globe
44 are making efforts to avoid a 1.5°C increase before 2025 [Christoff, 2016; Fuhrman *et al.*, 2023; Rogelj *et al.*, 2018]. To achieve this objective, efforts are being made to
45 mitigate further increases in atmospheric CO₂ by increasing carbon sinks and
46 decreasing carbon emissions. Increasing carbon sinks typically include carbon capture,
47 mineral carbon sequestration, and enhanced silicate mineral weathering [Beerling *et al.*, 2018; Fuhrman *et al.*, 2023; Hartmann and Kempe, 2008; Kealy, 2019; Zhu *et al.*,
48 2017]. Carbon emissions can be decreased by adopting renewable energy sources and
49 improving energy efficiency [Guan *et al.*, 2018; Orsini and Marrone, 2019].

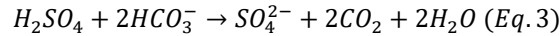
53 While green energy is increasingly replacing the traditional burning of fossil
54 fuels to reduce carbon emissions, more still needs to be done to explore ways to
55 reduce 'invisible' carbon sources associated with indirect CO₂-production pathways.
56 For example, the burning of coal is a complex process that not only oxidizes fossil
57 carbon into CO₂ but also releases elements such as sulfur into the environment [Ding
58 *et al.*, 2013; Kato and Akimoto, 1992; Zhao and Sun, 1986]. Sulfur, when involved in
59 subsequent chemical reactions, such as the chemical weathering of carbonates,
60 releases CO₂ into the atmosphere (Eqs 1-3), which is widely recognized as a
61 significant carbon source in the geological carbon cycle [Burke *et al.*, 2018; Calmels
62 *et al.*, 2007; M Torres *et al.*, 2016; M Torres *et al.*, 2014; M A Torres *et al.*, 2015].
63 Therefore, this study focuses on the invisible carbon source from sulfur (or sulfide)
64 oxidative weathering from the coal-burning process (Kato and Akimoto, 1992; Wu *et al.*, 2006; Zhao and Sun, 1986). Sulfide oxidative weathering can be described by the
65 generalized equation [Calmels *et al.*, 2007; M Torres *et al.*, 2014], which results in the
66 release of sulfuric acid:
67



68 The released sulfuric acid typically dissolves surrounding carbonate minerals:



69 Sulfuric acid can also react with bicarbonate in river water:



70 Both reactions lead to the release of CO₂ into the atmosphere [*Calmels et al.*,
71 2007; *M Torres et al.*, 2014].

72 Therefore, the burning of coal not only releases CO₂ directly but also results in
73 the production of SO₂, which can contribute to the formation of an "invisible" CO₂
74 source through Eqs. 2-3. This process is expected to result in a significantly higher
75 CO₂ flux, especially given the massive amounts of sulfur released by coal combustion
76 [*Dai et al.*, 2018; *Ding et al.*, 2013; *Kato and Akimoto*, 1992; *Lu et al.*, 2010; *D Wu et al.*,
77 *2006*; *Zhao and Sun*, 1986], which still accounts for more than half of China's
78 energy consumption [*Tang et al.*, 2019]. In fact, there has been a noticeable increase
79 in sulfate flux in coal-burning regions, with sulfate concentrations in the Yangtze
80 River increasing from 147 μM in 1978 to 285 μM in 2006 and 483 μM in 2011
81 [*Chetelat et al.*, 2008; *Xiaoqian Li et al.*, 2015; *Ming-hui et al.*, 1982]. Similarly, the
82 sulfate concentration in the Mississippi River has increased from about 154 μM before
83 industrialization to 611 μM in the 2010s [*Killingsworth and Bao*, 2015]. A large
84 amount of CO₂ has been released into the atmosphere through Equations 1, 2, and 3.
85 However, the flux of this anthropogenic-produced source of invisible CO₂ emissions
86 and its disturbance to the geological carbon cycle in catchments are still poorly
87 understood.

88 To fill this knowledge gap, we examined the Xijiang River basin in China, a
89 system that allowed us to evaluate the influence of invisible carbon from coal burning
90 at continental scales. This region was chosen due to its rapid industrialization and
91 significant coal consumption, making it an ideal place to conduct the study [*Xia Li*
92 *and Yeh*, 2004; *H-b Wang et al.*, 2019a; *S Wang et al.*, 2019b]. We mainly focused on
93 evaluating the changes in sulfate concentrations in the Xijiang River basin during the

94 period of rapid industrialization from the 1980s to 2010s to determine the contribution
95 of coal combustion to the sulfate flux. Additionally, this work calculated the invisible
96 carbon flux introduced by coal combustion based on riverine sulfate flux. Then we
97 propose a plan to reduce this source of atmospheric carbon and assess its expected
98 effectiveness in the Xijiang River basin and throughout China. Finally, we design a
99 prediction model based on coal consumption rates to estimate the flux of
100 anthropogenically-produced invisible carbon under different strategies in China from
101 1990 to 2050 to inform policy. Overall, this study aims to contribute to the global
102 effort to combat climate change by identifying invisible sources of carbon, evaluating
103 their impact on the carbon cycle, and proposing effective mitigation strategies to
104 reduce carbon emissions.

105 **Materials and Methods**

106 **Study Area**

107 This study focuses on the Xijiang River basin (Figure 1A, B), which was chosen
108 for its high degree of human activity, industrialization, fossil fuel consumption, and
109 significant occurrence of sulfuric acid rain [*Aas et al.*, 2007; *Ding et al.*, 2013]. The
110 Xijiang River basin is located in southern China, extending from eastern Yunnan
111 Province to southern Guangdong Province. The river, which originates from the
112 eastern foot of the Maxiong Mountain in Yunnan, flows east through Guangdong,
113 entering the Pearl River Delta east of Zhaoqing and exiting into the South China Sea
114 west of Macau. The basin has a drainage area of $3.53 \times 10^5 \text{ km}^2$, an average annual
115 temperature ranging from 14°C to 22°C, and mean annual precipitation ranging from
116 1000 mm to 2200 mm, with precipitation concentrated from April to September. The
117 basin's abundance of carbonate rocks, particularly limestone, is another crucial reason
118 for its selection, allowing for the observation of sulfuric acid weathering of carbonate
119 rocks. The basin has undergone extensive karst geomorphological processes at the
120 surface and underground due to approximately 44% of its composition being
121 carbonate rocks [*Gao et al.*, 2009; *Wei et al.*, 2013] (Figure 1).

122 The Xijiang River basin is one of China's most developed regions, with a

123 population of over 120 million. Coal accounts for 70% of China's energy budget
124 [Tang *et al.*, 2019], and the basin's industrialization has accelerated since the 1980s
125 with the implementation of China's reform and opening-up policy [P Wang *et al.*,
126 2013a; X Wang *et al.*, 2013b], resulting in the increased combustion of fossil fuels and
127 the release of substantial amounts of sulfur. The region is home to a variety of
128 industries, including coal-fired power plants, which have significantly increased in
129 number and size since the 2000s. This makes the Xijiang River basin an ideal case for
130 our study.

131 **Data Collection and Preprocessing**

132 Water chemistry data of the Xijiang River between 1980s~2000s was selected
133 from the United Nations Global Environmental Monitoring System (GEMS) Water
134 Program (<http://www.gemstat.org/>), which has collated and recorded high-quality data
135 sets of the most important rivers globally over the past few decades. These include pH,
136 temperature, electric conductivity (EC), and major ions (Ca^{2+} , Mg^{2+} , Na^+ , K^+ ,
137 alkalinity, Cl^- , SO_4^{2-}). The corresponding water temperature and discharge at the time
138 of sampling were also recorded. Sampling areas are shown in Figure 1. Based on
139 other previous works, we obtained the water chemistry data from 2000 to 2011 [Gao
140 *et al.*, 2009; Han *et al.*, 2019; Sun *et al.*, 2010; B Wang *et al.*, 2012; Wei *et al.*, 2013;
141 Xu and Liu, 2007; 2010]. The sampling areas of these works are also shown in Figure
142 1B.

143 **Model Design**

144 This study developed a comprehensive invisible carbon prediction model (ICPM)
145 based on coal combustion rates to estimate the flux of anthropogenically-produced
146 invisible carbon sources under different strategies in China from 1990 to 2050 to
147 estimate the invisible carbon emissions resulting from coal burning. The model takes
148 into account several factors, such as the reaction of acid rain with carbonate rocks,
149 SO_2 emissions from coal combustion, riverine sulfate flux, and potential CO_2
150 emissions (SI S1, 2, 3).

151 **Results**

152 **Sulfate Concentration Trends and Comparison**

153 The concentration of dissolved sulfate in the Xijiang River has been increasing
154 steadily over the three decades from the 1980s to the 2010s (Figure 2). Specifically,
155 the concentration of dissolved sulfate increased from 87 μM in 1985 to 358 μM in
156 2011, representing a more than 300% increase in 26 years. The rate of increase has
157 been particularly significant since the 2000s (Figure 2).

158 The sulfate concentration in the Xijiang River basin was compared to other major
159 rivers around the world using data from the year 2011. The results reveal that the
160 concentration of dissolved sulfate in the Xijiang River (358 μM) was significantly
161 higher than the volume-weighted average sulfate concentration (108 μM) of rivers
162 representing over 46% of the global water discharge [Burke *et al.*, 2018]. The Yamuna
163 and Ganges rivers, similar to the Xijiang, have also experienced significant increases
164 in sulfate concentrations, with concentrations of 360 μM and 370 μM , respectively.
165 These increases are likely due to intensive expansion of human and industrial
166 activities in those basins [Burke *et al.*, 2018; Rahaman *et al.*, 2012].

167

168 **Discussion**

169 **Coal Combustion & Sulfate Flux**

170 The sulfate concentration in the Xijiang River has increased by over 300% from
171 the 1980s to the 2010s (Figure 2), and due to its relatively high levels compared to
172 other major rivers worldwide, further investigation of the possible impact of
173 anthropogenic sulfate on the environment in this region is necessary. Firstly, it is
174 essential to distinguish the sources of sulfate, which is crucial for subsequent
175 evaluation and estimation of invisible carbon flux. Possible sources of sulfate in the
176 Xijiang River include natural sulfide weathering, evaporate dissolution within the
177 basin, as well as anthropogenic activities [Meybeck, 2003]. However, the sparsely
178 distributed evaporates in the upstream basin and the limited sulfides in the basin are
179 unlikely to cause such a significant change in sulfate concentration downstream,
180 ruling out the possibility of natural sources [Jiang *et al.*, 2018; Xiaoqian Li *et al.*,
181 2015] (Figure 1A). Rather anthropogenic activities, such as coal burning for industrial
182 or power generation purposes, have been shown in previous studies to significantly
183 contribute to the riverine sulfate flux in this area in recent years [Han and Liu, 2006;
184 Han *et al.*, 2019; Han *et al.*, 2011; J Liu *et al.*, 2022a; Q Wu *et al.*, 2012]. Moreover,
185 the growth trend of the sulfate concentration in the Xijiang River from 1985 to 2011
186 corresponds to the trend of coal burning in China (Figure 3A), which also implies the
187 contribution of coal burning to sulfate.

188 To investigate whether the rapid increase in sulfate in the Xijiang River between
189 the 1980s and 2010s is indeed mainly due to coal combustion, a correlation analysis
190 was conducted between the combustion of coal and sulfate concentration. Results
191 from Figure 3B demonstrate a robust positive correlation between the combustion of
192 coal in the Guangdong Province, mostly located in the study area, and dissolved
193 sulfate in the Xijiang River from 1995 to 2012, which provides further evidence that
194 the increase in sulfate concentration over the past three decades has come mainly
195 from coal combustion [Kuang, 2015]. Besides, the intercept of the fitted regression
196 equation indicates that the concentration of dissolved sulfate in the Xijiang River was

197 around 48.9 μM in the absence of coal combustion, which is consistent with previous
198 research that estimated the concentration of sulfate in the Xijiang River to be around
199 56.25 μM before the 1990s [*S-R Zhang et al.*, 2007].

200

201 **Sulfur-Driven CO₂ Emissions**

202 The previous section has shown that coal burning has significantly contributed
203 and elevated sulfate concentration in Xijiang River Basin. Notably, coal burning does
204 not only impact the sulfate flux in the river basin; it also leads to invisible carbon
205 emissions. Previous studies have shown that there is a large proportion of high-sulfur
206 coal in the Xijiang River basin, where over 95% of sulfur is present in the forms of
207 organic sulfur and pyrite, while the sulfate form of sulfur is only a small fraction [*Dai*
208 *et al.*, 2018; *Dai et al.*, 2017; *Jiang et al.*, 2018]. During high-temperature combustion,
209 organic sulfur and pyrite are released into the atmosphere as SO₂, forming acid rain.
210 This is supported by the recent occurrences of intense acid rain in the middle reaches
211 of the Xijiang River [*Aas et al.*, 2007; *Ding et al.*, 2013; *Hao et al.*, 2001].

212 Before or after entering the river, the sulfur from coal combustion reacts with
213 carbonates and/or bicarbonates in the form of sulfuric acid, releasing significant
214 amounts of CO₂ into the atmosphere (Eqs. 1-3), contributing to the "invisible carbon."
215 This phenomenon is particularly apparent in carbonate-rich river basins like the
216 Xijiang. We calculated the invisible CO₂ emission rate in the Xijiang River basin from
217 1995-2011 based on sulfate concentrations (Detailed calculation is in SI S4).
218 Specifically, the invisible CO₂ emission rates at Zhaoqing (Gaoyao) Station were
219 $4.18 \times 10^4 \text{ mol km}^{-2} \text{ a}^{-1}$ and $20.2 \times 10^4 \text{ mol km}^{-2} \text{ a}^{-1}$ in 1995 and 2011, respectively,
220 which offset all of the silicate weathering carbon sink ($5.49 \times 10^4 \text{ mol km}^{-2} \text{ a}^{-1}$) in 2011
221 (Figure 1B, 4A, Table S2) [*Gaillardet et al.*, 1999]. In other words, the invisible CO₂
222 flux to the atmosphere in the Xijiang River basin was 3.14 Mt in 2011 [*Xu and Liu,*
223 2010], indicating a significant carbon source that was previously overlooked. This
224 highlights the importance of considering not only direct emissions from fossil carbon
225 burning but also indirect emissions from secondary processes that are triggered by
226 human activities.

227 The increasing trend of invisible CO₂ rate from 1995-2011 (Figure 4A) shows
228 that the impact of this process, triggered by coal burning, is becoming more and more
229 significant. Importantly, this not only contributes to the overall sulfate flux in the
230 basin but also release CO₂ into the atmosphere, affecting the carbon cycle. This
231 observation corroborates previous studies that note that carbonate dissolution can
232 occur through sulfuric acid and carbonic acid [*M Torres et al.*, 2016] and the
233 proportion of carbonate dissolution from sulfuric acid is increasing in recent years
234 [*Han et al.*, 2019; *S-L Li et al.*, 2008; *Xu and Liu*, 2007]. The identified continuous
235 rise in anthropogenic invisible CO₂ emissions, resulting from the dissolution of
236 carbonate rocks and/or bicarbonates by sulfuric acid in the Xijiang River basin,
237 highlights the need to adopt more comprehensive and integrated approaches to
238 addressing carbon emissions and their impact on the environment.

239

240 **Mitigation Strategies**

241 The important yet often overlooked source of CO₂ emissions in the Xijiang River
242 has been linked to the presence of sulfuric acid. This source of carbon has shown a
243 steady increase, with a recorded value of 3.14 million tons in 2011, equal to the
244 carbon reduction achieved by more than 1000 fully-loaded 1.5 MW wind turbines
245 operating for one year [*Chen et al.*, 2011; *Kealy*, 2019]. To address this issue, one
246 potential solution is to implement flue gas desulfurization (FGD) (SI S1) [*Cordoba*,
247 2015; *van Ewijk and McDowall*, 2020; *B Wu et al.*, 2020]. Sulfur in coal mainly exists
248 in the form of organic sulfur and sulfides, with an average mass fraction of about 2%
249 [*Chou*, 2012]. Preventing sulfur from entering the terrestrial environment and
250 participating in subsequent chemical reactions could reduce the carbon emissions
251 from sulfuric acid dissolution of carbonate rocks. This can be achieved through FGD
252 [*Cordoba*, 2015].

253 It is important to note that many countries, including China, have implemented
254 measures to reduce SO₂ emissions. Under China's "Eleventh Five-Year Plan" since
255 around 2006, specific measures were introduced to reduce nitrogen and sulfur oxide
256 emissions, primarily aiming to protect the environment [*X Wang et al.*, 2013b; *Q*

257 *Zhang et al.*, 2012]. As evidenced by the case of the Xijiang River basin, these
258 measures have successfully reduced the flux of anthropogenic sulfur to the
259 atmosphere and consequently the anthropogenic invisible carbon source (Figure S2).

260 However, the reality is more complex. More than simply reducing SO₂ emissions
261 is needed to fully address the problem, as CO₂ may also be produced during
262 desulfurization, depending on the method used. Different flue gas desulfurization
263 (FGD) methods have varying carbon emissions patterns [*Cordoba*, 2015]. For
264 example, the limestone-gypsum method, also known as “wet limestone FGD,”
265 releases a large amount of CO₂ (SI S1, Eq. S1) [*Cordoba*, 2015]. In contrast, spray-dry
266 FGD systems do not have this issue (SI S1, Eq. S1) [*Cordoba*, 2015; *Zheng et al.*,
267 2002].

268 Thus, while FGD methods can effectively reduce SO₂ emissions, their
269 implementation may also lead to carbon emissions. Therefore, it is crucial to consider
270 the carbon emissions generated by various FGD methods when selecting the
271 appropriate technology. Here, the impact of two typical FGD methods (wet limestone
272 FGD and spray-dry FGD) on carbon emissions was examined to show their effects on
273 coal burning-invisible carbon emissions in 2030 and 2050 in China through our
274 invisible carbon prediction model (ICPM) (SI S3).

275

276 **Model Application and Policy Implication**

277 Based on the invisible carbon prediction model (ICPM), we calculated the
278 invisible carbon flux generated by different desulfurization methods and SO₂ removal
279 efficiency during coal burning in China from 1990 to 2050 (SI S1, 2). China's coal
280 consumption rate from 1990 to 2019 comes from the China Statistical Yearbook, and
281 the projected consumption of coal from 2030 to 2050 is sourced from the
282 International Energy Agency (IEA). Figure 4B shows the variation of carbon emission
283 flux caused by different desulfurization methods and SO₂ removal efficiency.

284 Firstly, ‘Wet limestone desulfurization,’ where the flue gas produced by coal
285 burning directly reacts with calcium carbonate, and the sulfur dioxide (SO₂) in the

286 flue gas is absorbed by calcium carbonate, can effectively prevent SO₂ from entering
287 the atmosphere (SI S1). However, when SO₂ reacts with calcium carbonate, it
288 produces large amounts of CO₂ (as shown in Equation S1), which is also considered
289 part of the invisible carbon emissions. Therefore, this FGD method does not reduce
290 invisible carbon emissions. If this method is applied, China's maximum invisible
291 carbon emission would equate to approximately 40 Mt in 2019 (Figure 4B).

292 The other desulfurization method we selected for model calculation is 'spray-dry
293 FGD systems' (SI S1) [Cordoba, 2015; X Liu et al., 2022b; Zheng et al., 2002]. The
294 invisible carbon emission introduced by coal burning under this desulfurization
295 method is significantly lower than that of 'wet limestone FGD'. Moreover, with the
296 increase of the SO₂ removal efficiency, the invisible carbon emission is significantly
297 reduced (Figure 4B). If the SO₂ removal efficiency reaches 75%, China's invisible
298 carbon emissions will decrease by 27.8 Mt of CO₂ in 2019, reducing to 4.9 Mt by the
299 year 2050 (Figure 4B).

300 The estimated invisible carbon emissions under the two different desulfurization
301 methods and SO₂ removal efficiency in China from 1990 to 2050 highlight the
302 importance of selecting appropriate desulfurization methods. This demonstrates the
303 potential benefits of implementing desulfurization methods, such as spray-dry FGD
304 systems, that do not generate additional 'invisible' CO₂, thereby contributing to global
305 efforts to mitigate climate change. By adopting the most suitable desulfurization
306 methods and increasing the SO₂ removal efficiency, China can significantly reduce its
307 invisible carbon emissions during coal burning, moving towards a more sustainable
308 future by addressing two of the Sustainable Development Goals of the United Nations
309 (namely 7 – Affordable and Clean Energy and 13 – Climate Action).

310

311 **Conclusion**

312

313 This work has revealed the significant contribution of coal combustion to the
314 sharp increase in riverine sulfate concentration over time in the Xijiang River basin,

315 as well as the invisible carbon emission originating from the reaction of sulfuric acid
316 with carbonates and/or bicarbonates. An upward trend in the invisible carbon flux is
317 evident from 1995-2011, underscoring the growing significance of this process. This
318 rising trend in anthropogenic invisible CO₂ emissions has profound implications for
319 our understanding of carbon emissions and their environmental impacts.

320 Moreover, the implementation of Flue Gas Desulfurization (FGD) technologies
321 emerges as a potential solution to mitigate this issue. Our invisible carbon prediction
322 model (ICPM) reveals that the choice of desulfurization method and the SO₂ removal
323 efficiency significantly impact the carbon emission flux. For example, using a
324 desulfurization method that does not produce additional CO₂, such as spray dry FGD
325 systems, and increasing the SO₂ removal efficiency could substantially reduce China's
326 invisible carbon emissions by 2050.

327 In conclusion, the study of the Xijiang River basin has underscored the pressing
328 need to address not only direct emissions from fossil fuel combustion but also indirect
329 emissions arising from secondary processes triggered by human activities. The
330 selection of appropriate desulfurization methods and optimization of SO₂ removal
331 efficiency can help to reduce invisible carbon emissions, thereby contributing to the
332 global effort to mitigate climate change. As we continue to refine our understanding
333 of these complex processes, we are better equipped to design and implement
334 strategies to reduce carbon emissions and foster a more sustainable future.

335

336 **Acknowledgments**

337

338 We would like to thank Prof. Junfeng Ji and Prof. Wei Li of Nanjing University
339 for their helpful suggestions in the design of this study. Special thanks to Dr. Gen Li
340 from UC Santa Barbara, for the valuable input on the revision and enhancement of the
341 manuscript. This work was supported by the Natural Science Foundation of China
342 (No. 41991252 and 41991321).

343

344 **Data Availability Statement**

345

346 Data used in this study can be accessed through this link:

347 <https://figshare.com/s/fe51a91d60cfda01a78>

348

349 **Reference**

- 350 Aas, W. et al., 2007. Air concentrations and wet deposition of major inorganic ions at five
351 non-urban sites in China, 2001–2003. *Atmospheric Environment*, 41(8): 1706-1716.
- 352 Andrews, T., Forster, P.M., 2008. CO2 forcing induces semi-direct effects with consequences
353 for climate feedback interpretations. *Geophysical Research Letters*, 35(4).
- 354 Beerling, D.J. et al., 2018. Farming with crops and rocks to address global climate, food and
355 soil security. *Nature Plants*, 4(3): 138-147.
- 356 Berrang-Ford, L. et al., 2019. Tracking global climate change adaptation among governments.
357 *Nature Climate Change*, 9(6): 440-449.
- 358 Burke, A. et al., 2018. Sulfur isotopes in rivers: Insights into global weathering budgets, pyrite
359 oxidation, and the modern sulfur cycle. *Earth and Planetary Science Letters*, 496:
360 168-177.
- 361 Calmels, D., Gaillardet, J., Brenot, A., France-Lanord, C., 2007. Sustained sulfide oxidation by
362 physical erosion processes in the Mackenzie River basin: Climatic perspectives.
363 *Geology*, 35: 1003-1006.
- 364 Charney, J.G. et al., 1979. Carbon dioxide and climate: a scientific assessment. National
365 Academy of Sciences, Washington, DC.
- 366 Chen, G.Q., Yang, Q., Zhao, Y.H., 2011. Renewability of wind power in China: A case study of
367 nonrenewable energy cost and greenhouse gas emission by a plant in Guangxi.
368 *Renewable and Sustainable Energy Reviews*, 15(5): 2322-2329.
- 369 Chetelat, B. et al., 2008. Geochemistry of the dissolved load of the Changjiang Basin rivers:
370 Anthropogenic impacts and chemical weathering. *Geochimica et Cosmochimica Acta*,

371 72(17): 4254-4277.

372 Chou, C.-L., 2012. Sulfur in coals: A review of geochemistry and origins. International Journal
373 of Coal Geology, 100: 1-13.

374 Christoff, P., 2016. The promissory note: COP 21 and the Paris Climate Agreement.
375 Environmental Politics, 25(5): 765-787.

376 Cordoba, P., 2015. Status of Flue Gas Desulphurisation (FGD) systems from coal-fired power
377 plants: Overview of the physic-chemical control processes of wet limestone FGDs.
378 Fuel, 144: 274-286.

379 Dai, S. et al., 2018. The occurrence of buddingtonite in super-high-organic-sulphur coals from
380 the Yishan Coalfield, Guangxi, southern China. International Journal of Coal Geology,
381 195: 347-361.

382 Dai, S. et al., 2017. Anomalies of rare metals in Lopingian super-high-organic-sulfur coals from
383 the Yishan Coalfield, Guangxi, China. Ore Geology Reviews, 88: 235-250.

384 Ding, H.U., Lang, Y.-C., Liu, C.-Q., Liu, T.-Z., 2013. Chemical characteristics and
385 $\delta^{34}\text{S}$ – SO_4^{2-} of acid rain:
386 Anthropogenic sulfate deposition and its impacts on CO_2 consumption in
387 the rural karst area of southwest China. GEOCHEMICAL JOURNAL, 47(6): 625-638.

388 Fuhrman, J. et al., 2023. Diverse carbon dioxide removal approaches could reduce impacts on
389 the energy–water–land system. Nature Climate Change, 13(4): 341-350.

390 Gao, Q. et al., 2009. Chemical weathering and CO_2 consumption in the Xijiang River basin,
391 South China. Geomorphology, 106(3): 324-332.

392 Guan, D. et al., 2018. Structural decline in China's CO_2 emissions through transitions in

393 industry and energy systems. *Nature Geoscience*, 11(8): 551-555.

394 Han, G., Liu, C.-Q., 2006. Strontium isotope and major ion chemistry of the rainwaters from
395 Guiyang, Guizhou Province, China. *Science of The Total Environment*, 364(1):
396 165-174.

397 Han, G., Tang, Y., Wu, Q., Liu, M., Wang, Z., 2019. Assessing Contamination Sources by
398 Using Sulfur and Oxygen Isotopes of Sulfate Ions in Xijiang River Basin, Southwest
399 China. *Journal of Environmental Quality*, 48(5): 1507-1516.

400 Han, G., Wu, Q., Tang, Y., 2011. Acid rain and alkalization in southwestern China: chemical
401 and strontium isotope evidence in rainwater from Guiyang. *Journal of Atmospheric
402 Chemistry*, 68(2): 139-155.

403 Hao, J., Duan, L., Zhou, X., Fu, L., 2001. Application of a LRT Model to Acid Rain Control in
404 China. *Environmental Science & Technology*, 35(17): 3407-3415.

405 Hartmann, J., Kempe, S., 2008. What is the maximum potential for CO₂ sequestration by
406 “stimulated” weathering on the global scale? *Naturwissenschaften*, 95(12):
407 1159-1164.

408 Jiang, H., Li, W., Zhao, T., Sun, H., Xu, Z., 2018. Water geochemistry of rivers draining
409 karst-dominated regions, Guangxi province, South China: Implications for chemical
410 weathering and role of sulfuric acid. *Journal of Asian Earth Sciences*, 163: 152-162.

411 Kato, N., Akimoto, H., 1992. Anthropogenic emissions of SO₂ and NO_x in Asia: emission
412 inventories. *Atmospheric Environment. Part A. General Topics*, 26(16): 2997-3017.

413 Kealy, T., 2019. A review of CO₂ emission reductions due to wind turbines using energy
414 benchmarks: a focus on the Irish electrical energy market. *International Journal of*

415 Global Warming, 19: 267.

416 Killingsworth, B.A., Bao, H., 2015. Significant Human Impact on the Flux and $\delta^{34}\text{S}$ of Sulfate
417 from the Largest River in North America. *Environmental Science & Technology*, 49(8):
418 4851-4860.

419 Li, S.-L., Calmels, D., Han, G., Gaillardet, J., Liu, C.-Q., 2008. Sulfuric acid as an agent of
420 carbonate weathering constrained by $\delta^{13}\text{C}_{\text{DIC}}$: Examples from Southwest China.
421 *Earth and Planetary Science Letters*, 270(3): 189-199.

422 Li, X., Gan, Y., Zhou, A., Liu, Y., 2015. Relationship between water discharge and sulfate
423 sources of the Yangtze River inferred from seasonal variations of sulfur and oxygen
424 isotopic compositions. *Journal of Geochemical Exploration*, 153: 30-39.

425 Li, X., Yeh, A.G.-O., 2004. Analyzing spatial restructuring of land use patterns in a fast growing
426 region using remote sensing and GIS. *Landscape and Urban Planning*, 69(4):
427 335-354.

428 Liu, J., Han, G., Zhang, Q., Liu, M., Li, X., 2022a. Stable Isotopes and Bayesian Tracer Mixing
429 Model Reveal Chemical Weathering and CO_2 Release in the Jiulongjiang River Basin,
430 Southeast China. *Water Resources Research*, 58(9): e2021WR031738.

431 Liu, X., Wei, Y., Ji, J., 2022b. Quantifying the “Water–Carbon–Sulfur” Nexus for Coal Power
432 Plants in China. *Sustainability*, 14: 3675.

433 Lu, Z. et al., 2010. Sulfur dioxide emissions in China and sulfur trends in East Asia since 2000.
434 *Atmos. Chem. Phys.*, 10(13): 6311-6331.

435 Meybeck, M., 2003. 5.08 - Global Occurrence of Major Elements in Rivers. In: Holland, H.D.,
436 Turekian, K.K. (Eds.), *Treatise on Geochemistry*. Pergamon, Oxford, pp. 207-223.

437 Ming-hui, H., Stallard, R.F., Edmond, J.M., 1982. Major ion chemistry of some large Chinese
438 rivers. *Nature*, 298(5874): 550-553.

439 Orsini, F., Marrone, P., 2019. Approaches for a low-carbon production of building materials: A
440 review. *Journal of Cleaner Production*, 241.

441 Rahaman, W., Singh, S.K., Shukla, A.D., 2012. Rhenium in Indian rivers: Sources, fluxes, and
442 contribution to oceanic budget. *Geochemistry, Geophysics, Geosystems*, 13(8).

443 Rogelj, J. et al., 2018. Scenarios towards limiting global mean temperature increase below 1.5
444 degrees C. *Nature Climate Change*, 8(4): 325-+.

445 Sun, H., Han, J., Li, D., Zhang, S., Lu, X., 2010. Chemical weathering inferred from riverine
446 water chemistry in the lower Xijiang basin, South China. *Science of The Total
447 Environment*, 408(20): 4749-4760.

448 Tang, L. et al., 2019. Substantial emission reductions from Chinese power plants after the
449 introduction of ultra-low emissions standards. *Nature Energy*, 4(11): 929-938.

450 Torres, M. et al., 2016. The acid and alkalinity budgets of weathering in the Andes–Amazon
451 system: Insights into the erosional control of global biogeochemical cycles, 450.

452 Torres, M., West, A.J., Li, G., 2014. Sulphide oxidation and carbonate dissolution as a source
453 of CO₂ over geological timescales. *Nature*, 507: 346-9.

454 Torres, M.A., West, A.J., Clark, K.E., 2015. Geomorphic regime modulates hydrologic control
455 of chemical weathering in the Andes–Amazon. *Geochimica et Cosmochimica Acta*,
456 166: 105-128.

457 van Ewijk, S., McDowall, W., 2020. Diffusion of flue gas desulfurization reveals barriers and
458 opportunities for carbon capture and storage. *Nature Communications*, 11(1): 4298.

459 Wang, B. et al., 2012. Distinct patterns of chemical weathering in the drainage basins of the
460 Huanghe and Xijiang River, China: Evidence from chemical and Sr-isotopic
461 compositions. *Journal of Asian Earth Sciences*, 59: 219-230.

462 Wang, H.-b. et al., 2019a. Arsenic concentration, speciation, and risk assessment in
463 sediments of the Xijiang River basin, China. *Environmental Monitoring and
464 Assessment*, 191(11).

465 Wang, P., Wu, W., Zhu, B., Wei, Y., 2013a. Examining the impact factors of energy-related
466 CO₂ emissions using the STIRPAT model in Guangdong Province, China. *Applied
467 Energy*, 106: 65-71.

468 Wang, S., Wang, J., Li, S., Fang, C., Feng, K., 2019b. Socioeconomic driving forces and
469 scenario simulation of CO₂ emissions for a fast-developing region in China. *Journal of
470 Cleaner Production*, 216: 217-229.

471 Wang, X. et al., 2013b. Reductions in sulfur pollution in the Pearl River Delta region, China:
472 Assessing the effectiveness of emission controls. *Atmospheric Environment*, 76:
473 113-124.

474 Wei, G. et al., 2013. Seasonal changes in the radiogenic and stable strontium isotopic
475 composition of Xijiang River water: Implications for chemical weathering. *Chemical
476 Geology*, 343: 67-75.

477 Wu, B. et al., 2020. Non-Negligible Stack Emissions of Noncriteria Air Pollutants from
478 Coal-Fired Power Plants in China: Condensable Particulate Matter and Sulfur Trioxide.
479 *Environmental Science & Technology*, 54(11): 6540-6550.

480 Wu, D., Tie, X.X., Deng, X.J., 2006. Chemical characterizations of soluble aerosols in southern

481 China. *Chemosphere*, 64(5): 749-757.

482 Wu, Q., Han, G., Tao, F., Tang, Y., 2012. Chemical composition of rainwater in a karstic
483 agricultural area, Southwest China: The impact of urbanization. *Atmospheric*
484 *Research*, 111: 71-78.

485 Xu, Z., Liu, C.-Q., 2007. Chemical weathering in the upper reaches of Xijiang River draining
486 the Yunnan–Guizhou Plateau, Southwest China. *Chemical Geology*, 239(1): 83-95.

487 Xu, Z., Liu, C.-Q., 2010. Water geochemistry of the Xijiang basin rivers, South China:
488 Chemical weathering and CO₂ consumption. *Applied Geochemistry*, 25(10):
489 1603-1614.

490 Zhang, Q., He, K., Huo, H., 2012. Cleaning China's air. *Nature*, 484(7393): 161-162.

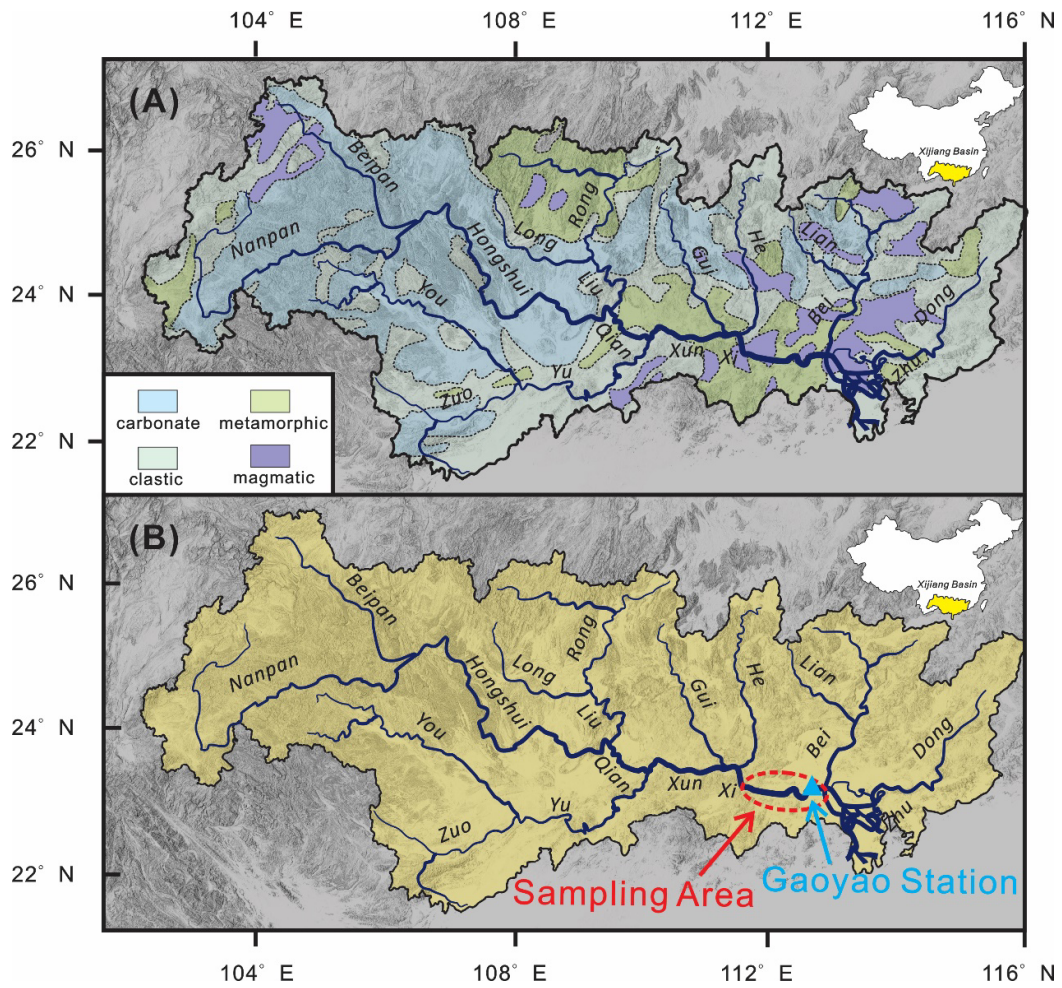
491 Zhang, S.-R. et al., 2007. Water chemistry of the Zhujiang (Pearl River): Natural processes
492 and anthropogenic influences. *Journal of Geophysical Research: Earth Surface*,
493 112(F1).

494 Zhao, D., Sun, B., 1986. Atmospheric Pollution from Coal Combustion in China. *Journal of the*
495 *Air Pollution Control Association*, 36(4): 371-374.

496 Zheng, Y., Kiil, S., Johnsson, J.E., Zhong, Q., 2002. Use of spray dry absorption product in wet
497 flue gas desulphurisation plants: pilot-scale experiments. *Fuel*, 81(15): 1899-1905.

498 Zhu, C. et al., 2017. CO₂ absorption and magnesium carbonate precipitation in MgCl₂–NH₃–
499 NH₄Cl solutions: implications for carbon capture and storage. *Minerals*, 7(9): 172.

500

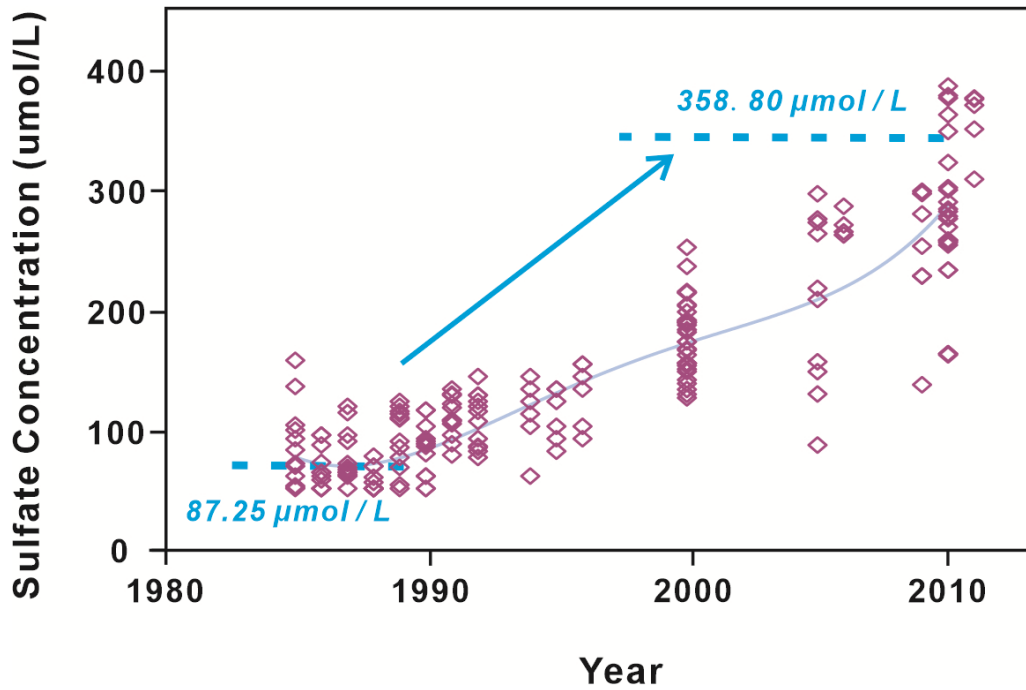


501

502 **Figure 1. (A) Geological settings and (B) Sampling areas in Xijiang**
 503 **River Basin. The sampling positions of all data are located in the red**
 504 **ellipse area. The blue triangle represents the position of Gaoyao**
 505 **Station.**

506

507



508

509 **Figure 2. Interannual variation of sulfate concentration in the**
510 **Xijiang River basin from the 1980s to 2010s. The “purple diamonds”**
511 **are sulfate concentrations of the lower reaches of the Xijiang River**
512 **from the 1980s to the 2010s. The “blue dotted lines” are the average**
513 **sulfate concentrations in 1985 and 2011, which are 87.25 uM and**
514 **358.80 uM, respectively. The “blue arrows” represent the trend of**
515 **change.**

516

517

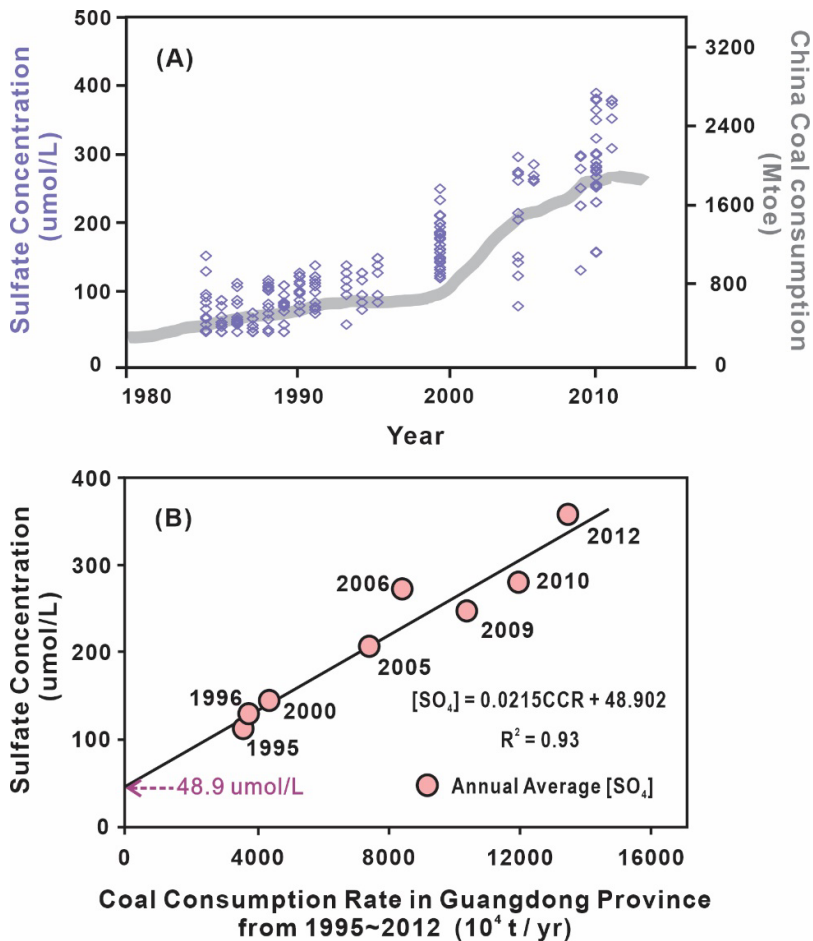
518

519

520

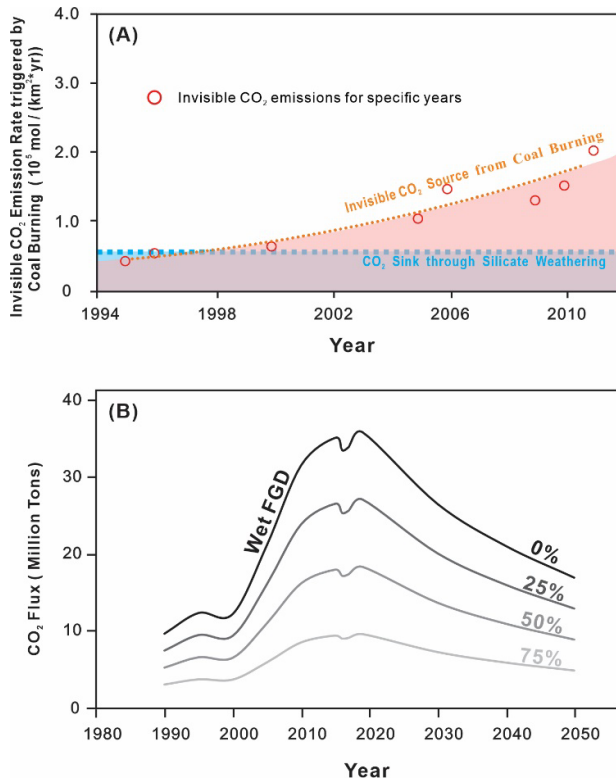
521

522



523

524 **Figure 3. (A) Interannual variation of sulfate concentration in the**
 525 **Xijiang River basin (purple diamonds) and interannual variation of**
 526 **sulfate concentration in the Xijiang River basin (purple diamonds) and interannual variation of**
 527 **coal consumption in China (gray curve). Data for interannual**
 528 **variation of coal consumption in China were collected from the**
 529 **China Statistical Yearbook. (B) Positive correlation between coal**
 530 **consumption Rate (CCR) in the Guangdong Province from 1995 to**
 531 **2012 and dissolved sulfate in the Xijiang River. The purple dotted**
 532 **arrow indicates the longitudinal intercept of the fitted linear equation,**
 533 **representing the sulfate concentration in the lower reaches of the**
Xijiang River without coal burning.



534

535 **Figure 4. (A) Comparison of invisible carbon source induced by coal**
 536 **burning with natural silicate chemical weathering carbon sink in the**
 537 **Xijiang River basin. The blue area represents the silicate chemical**
 538 **weathering carbon sink, and light orange area represents the**
 539 **invisible carbon source caused by coal burning. (B) The annual flux**
 540 **of invisible carbon emissions induced by coal burning in China from**
 541 **1990 to 2050 with different desulfurization methods and SO₂ removal**
 542 **efficiency. The top black line represents the invisible carbon**
 543 **emissions after wet limestone FGD application. 0, 25%, 50%, and**
 544 **75%, respectively, represent the invisible carbon emissions caused by**
 545 **coal burning after the application of “non-carbon emission FGD”**
 546 **with an SO₂ removal efficiency of 0, 25%, 50%, and 75%.**